

Hyperspectral proximal sensing for carbonate rocks characterization in the SWIR (Short-Wave Infrared)

Teledetección hiperspectral de proximidad para la caracterización de rocas carbonatadas en el infrarrojo de onda corta (SWIR)

Indira Rodríguez^{*1}, Eduardo García-Meléndez¹, Montserrat Ferrer-Julià⁽¹⁾, Wim Bakker², Juncal A. Cruz¹, and Antonio Espín de Gea³

¹ Grupo de Investigación Geología Ambiental, Cuaternario y Geodiversidad (Q-GEO), Facultad de Ciencias Biológicas y Ambientales. Universidad de León. Campus de Vegazana, s/n, 24071, León.

iroda@unileon.es, egarm@unileon.es, mferj@unileon.es, jcrum@unileon.es

² Department of Applied Earth Sciences, Faculty of Geo information Science & Earth Observation (ITC), University Twente, Hallenweg 8, 7522 NH Enschede, The Netherlands. w.h.bakker@utwente.nl

³ Unidad Tecnológica Geológico-Minera del Centro Tecnológico del Mármol, Piedra y Materiales (CTM). Ctra. de Murcia s/n. 30430, Cehegín (Murcia, España). antonio.espin@ctmarmol.es

^{*}Corresponding author

ABSTRACT

In this work proximal hyperspectral images are used to make a compositional map of one sample of ornamental carbonate rock (formed by variable content of dolomite and calcite) in terms of mineralogical composition. The hyperspectral dataset consists of a total number of 278 bands corresponding to the short-wave infrared (SWIR) wavelengths. After visual analysis and interpretation, 8 points or pixels were selected as reference spectra for image classification through the Spectral Angle Mapper (SAM) algorithm. The results show the spatial distribution of calcite and dolomite based on their characteristic and diagnostic absorption features (at 2335 and 2315 nm respectively), and areas with different proportions of calcite and dolomite mixture, and the presence of carbonates and clay mineral mixtures. The applied technique demonstrates the potential of hyperspectral proximal sensing procedures for mineral characterization of samples in the laboratory, expanding the application for the analysis and interpretation in field outcrops.

Key-words: Mineral composition, imaging spectrometry, spectral signature.

RESUMEN

En este trabajo se utilizan imágenes hiperspectrales de Teledetección de proximidad para realizar un mapa composicional de una muestra de roca carbonatada de uso ornamental (formada por un contenido variable de calcita y dolomita) en términos de composición mineralógica. El conjunto de datos hiperspectrales consta de un número total de 278 bandas correspondientes a las longitudes de onda del infrarrojo de onda corta (SWIR). Después del análisis e interpretación visual, se seleccionaron 8 puntos o píxeles como espectros de referencia para la clasificación de imágenes mediante el algoritmo Spectral Angle Mapper (SAM). Los resultados muestran la distribución espacial de calcita y dolomita en función de rasgos de absorción diagnósticos (en 2335 y 2315 nm respectivamente), y áreas con diferentes proporciones de mezcla de calcita y dolomita, así como la presencia de mezclas de carbonatos con minerales arcillosos. La técnica aplicada demuestra el potencial de los procedimientos de teledetección hiperspectral de proximidad para la caracterización mineral de muestras en el laboratorio, ampliando la aplicación para el análisis y la interpretación en afloramientos de campo.

Palabras clave: Composición mineral, espectrometría de imágenes, firma espectral.

Geogaceta, 77 (2025), 55-58

<https://doi.org/10.55407/geogaceta108997>

ISSN (versión impresa): 0213-683X

ISSN (Internet): 2173-6545

Fecha de recepción: 26/07/2024

Fecha de revisión: 30/10/2024

Fecha de aceptación: 29/11/2024

Introduction

Remote sensing is the science of acquiring, processing, and interpreting images and related data, acquired from aircraft, satellites, UAVs and ground based sensors that record the interaction between matter and electromagnetic energy. High spectral resolution on airborne and satellite spectrophotometers, as well as hyperspectral cameras for UAVs, ground and laboratory has enlarged the mapping capabilities of remote sensing data. These sensors developed with the use of AVIRIS data operating since 1988, and later with other sensors such as Hy-

Map. Advances on data calibration and the development of algorithms that allow the information extraction from a large number of spatial spectral data based on field and laboratory spectra, encouraged the development of applications on environmental and geological issues.

Imaging spectrometry (also known as hyperspectral imaging - HSI), simultaneous measurements of spectra and images in up to hundreds of spectral channels or bands, is a proven technology for identifying and mapping minerals based on their reflectance or emissivity signatures (Goetz *et al.*, 1985). The analysis of imaging spectrometer data enables the extraction of a detail-

led spectrum for each pixel in the image. Therefore, the pixels of a hyperspectral image contains the continuous reflectance spectrum of the corresponding area, according to its spectral resolution (Fig. 1), and the spectra acquired is the mixture of the spectral response of all the components on the analyzed surface. In the case of proximal sensing of rock samples, the analysis of each spectrum allows knowing the mineralogical composition of major components, and in some cases the quantification of each mineral phase, which implies that the mapping of the mineralogical composition can be done from a hyperspectral image (Goetz *et al.*, 1985).

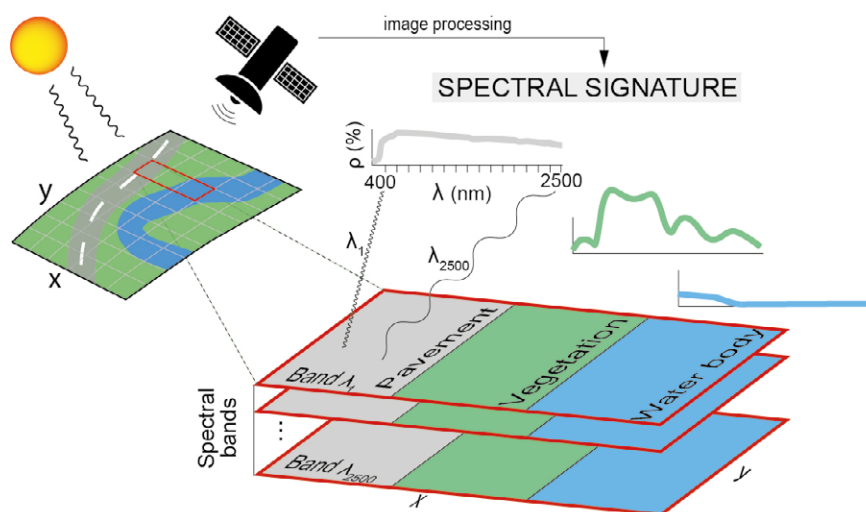


Fig. 1.- Acquisition of a hyperspectral imaging dataset. Each pixel in the image has an associated reflectance spectrum characteristic of the mixture of surface materials that include it (ρ : reflectance and λ : wavelength). See color figure on the web.

Fig. 1.- Esquema de la obtención y el tratamiento de un conjunto de datos de imágenes hiperespectrales. Cada píxel de la imagen tiene asociado un espectro de reflectancia característico de la mezcla de materiales superficiales que lo incluyen (ρ : reflectancia y λ : longitud de onda). Ver figura en color en la web.

High spectral resolution reflectance spectra collected by imaging spectrometers enable the direct identification of individual materials, including minerals, and in some cases, the determination of their abundance, based on their reflectance characteristics. There are a growing number of papers that are focused on the mapping of the mineral composition of the Earth surface by using this methodology (Riaza *et al.*, 2011). In recent years, proximal imaging spectroscopy is a new development as an alternative since it can assess the spectral rock constituents. This technique allows acquiring quantitative mineral data at the fine spatial, spectral and temporal resolutions (Murphy *et al.*, 2014; Zaini *et al.*, 2014; Boesche *et al.*,

2015; Krupnik and Khan, 2019, Alonso de Linaje and Khan, 2017, among others).

Reflectance spectra of minerals are dominated in the VNIR (visible/near infrared) wavelength range of the electromagnetic spectrum by the presence or absence of transition metal ions (such as Fe, Cr, Co, Ni) resulting in absorption features due to electronic processes. On the other hand, the presence or absence of water and hydroxyl, carbonate and sulfate, determines absorption features in the SWIR (short wave infrared) region due to molecular vibrational processes (Hunt, 1977). Small differences in absorption band position and shape in the

VNIR-SWIR (or emissivity in the LWIR, long wave infrared) are correlated with mineral compositional differences and variability (Kruse *et al.*, 1993)

The main mineralogical compositions of carbonate rocks are carbonate minerals consisted of calcite (CaCO_3) and dolomite ($\text{CaMg}(\text{CO}_3)_2$). The technique of infrared spectroscopy, based on spectral shapes and characteristic features, has been extensively used for many decades to determine the mineral chemistry and composition of carbonate rocks (Gaffey, 1984). The diagnostic absorption features of carbonate minerals in the SWIR region are determined by vibrational processes of the carbonate ions (CO_3^{2-}). These minerals have two distinctive spectral absorption features which positions are centered

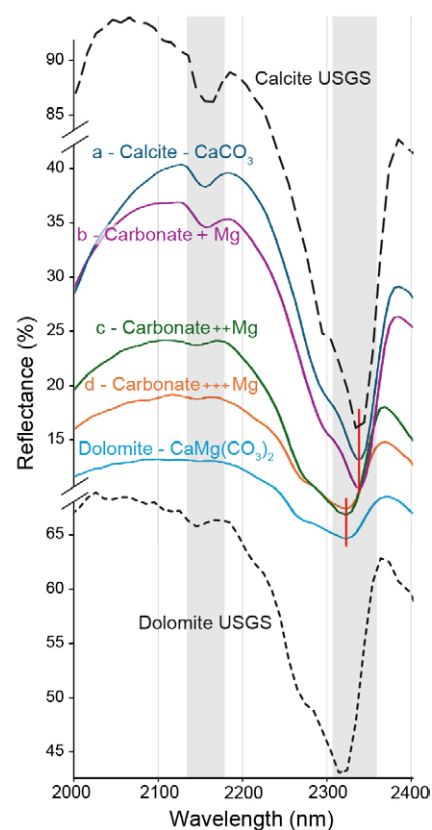


Fig. 4.- Spectral curves corresponding to the pixels belonging to areas of the rock sample where color varies gradually. The + symbols correspond to the proportion of Mg, from lower (+) to higher (+++), in the carbonate mixture (calcite/dolomite). The spectral curves of pure calcite and dolomite from the USGS spectral library are added. See color figure on the web.

Fig. 4.- Gráfico que muestra las curvas espectrales correspondientes a los píxeles pertenecientes a zonas de la muestra en las que el color varía gradualmente. Los símbolos de + corresponden a la proporción de mg, de menor (+) a mayor (+++), en la mezcla de carbonatos (calcita/dolomita). Se añaden las curvas espectrales de calcita y dolomita puras de la biblioteca del USGS. Ver figura en color en la web.

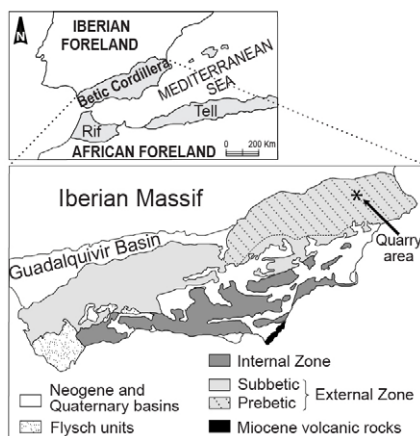


Fig. 2.- Location of the quarry where rocks used in this work were extracted.

Fig. 2.- Localización de la cantera donde se extrajeron las rocas utilizadas en este trabajo.

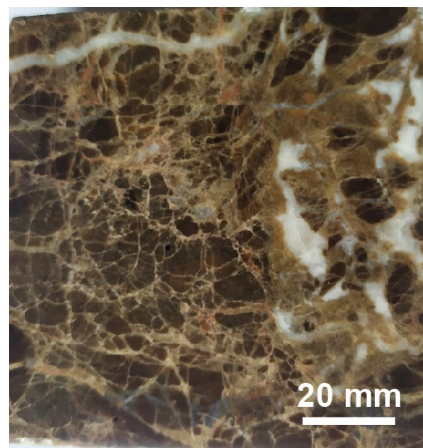


Fig. 3.- Photograph of the Marrón Imperial sample used in this work. See color figure on the web.

Fig. 3.- Fotografía de la muestra de Marrón Imperial utilizada en este trabajo. Ver figura en color en la web.

at 2500–2550 nm and 2300–2350 nm in the SWIR region (Clark, 1999; Gaffey, 1984; Hunt and Salisbury, 1971; van der Meer, 1995; Zaini et al., 2014, among others). Additional carbonate vibrational features or weak absorption features in the SWIR region occur around 2230–2270 nm, 2120–2160 nm, 1970–2200 nm, 1850–1870 nm and 1750–1800 nm. The presence of clay minerals in an intimate mixture with carbonates is usually indicated by a vibrational absorption feature around 2200 nm and 2300 nm caused by the bonding between OH groups with Al or Mg, respectively, in the octahedral layers of the phyllosilicates.

The objectives of this work are the spectral characterization and elaboration of a compositional map of two fragments of the so-called *Marrón Imperial* ornamental rock and to show the mapping potential of proximal hyperspectral imagery for the spatial compositional characterization of rock samples. The *Marrón Imperial* belongs to the Cuchillo dolostones and the las Moratillas limestones (Cenomanian-Turonian, Upper Cretaceous), exploited in the Prebetic Domain (Fig. 2) of the Betic Cordilleras (Murcia Province). These rocks consist of recrystallized dolostones, and limestones associated with a NNE-SSW morpho-structural alignment (Baena, 1974; Jerez et al. 1974). The rock as a whole has clean calcite veinlets frequently microcrystalline that, together with the calcite coming from karstification processes, are the cause of the multicolored reticulated structure characteristic of the rock (Fig. 3).

Method

In order to identify and map the mineralogical composition of selected sedimentary samples, hyperspectral images of two rock samples were obtained using a lab-based short-wave infrared (SWIR) hyperspectral sensor and treated with the ENVI 5.2 software.

Images were acquired by a hyperspectral imager of spectral imaging LTD (SPECIM) with a spatial resolution of 0.256 mm and a spectral resolution of 12 nm, recording a total of 288 spectral bands. In this way, for each pixel a curve with 288 points is constructed in which the absorption features of each mineral, whose surface includes several pixels, are distinguished (Fig. 1).

Several pre-processing steps were applied to the spectral data in order to obtain reflectance images and decrease spectral bands with errors maintaining a final data set of 278 bands. In the first step images were visually analyzed through several color compositions in order to detect the spatial distribution of different mineral concentrations. Afterwards, the spectral curve of representative pixels from different visually distinguished areas are compared with the spectral response of minerals from the USGS spectral library (Kokaly et al. 2017). These representative pixels were selected for image classification (Fig.4). Among the several image classification algorithms the *Spectral Angle Mapper* (SAM) was used because is based on the spectral similarity between reflectance spectral of image pixels with refe-

rence spectra with known materials from spectral libraries (Kruse et al., 1993). The algorithm determines the spectral similarity between the spectra by calculating the angle between them and treating them as vectors in a space where the dimensionality corresponds to the number of bands. Smaller angles indicate a closer match to the reference spectrum. The value of the angle used has been 0.13 radians. Pixels further away than the specified maximum angle threshold in radians are not classified. The results were validated through the comparison of the spectral response of the units mapped with the minerals of the USGS spectral library.

Results and discussion

The results show a compositional map representing the spatial distribution of the previous spectral curves indicating the mineral compositional variability (Fig. 5).

Eight units have been mapped based on the eight spectral chosen signatures as representative of the different mineral composition variability. These signatures are characterized by features representing absorption peaks whose position and shape are related to the identification of the mineral, and depth to the quantification estimation (Fig.4).

An important factor determining the position of the carbonate absorption features is cation mass, playing the radius a secondary role (Gaffey, 1984). Thus, the presence of Mg in dolomite provokes a shift of the absorption feature to shorter wavelengths (2315nm) compared to the one of calcite (2335nm).

In the resulting classification, the areas represented in greenish colours in figure 5, correspond to dolomites with variable amounts of Mg or a calcite/dolomite mixture, depicted in figure 4 as b, c, d and e.

Reflectance spectra are extremely sensitive to the presence of water, showing two strong absorption features at around 1400 nm and 1900 nm, if present. Bound water is indicated as spectral features at 1400 nm and at 1900 nm, on the other hand, unbound water is only represented at 1900 nm.

Most of the image reflectance spectra shows features at both around 1400 nm and 1900 nm. The features at 1400 nm are less developed (Fig.5), and at some points, almost indistinguishable. The-

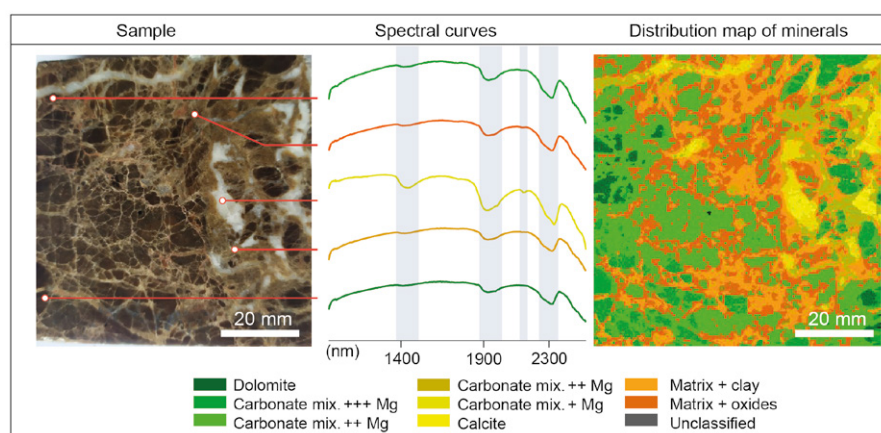


Fig. 5.- Comparison between the photograph of the sample used in this study and the mineral distribution map obtained from the spectral curves of the most representative pixels. The + symbols correspond to the proportion of Mg, from lower (+) to higher (+++), in the carbonate mixture. See color figure on the web.

Fig. 5.- Comparación entre la fotografía de la muestra utilizada en este estudio y el mapa de distribución de minerales obtenido a partir del estudio de las curvas espectrales de las zonas más representativas. Los símbolos de + corresponden a la proporción de mg, de menor (+) a mayor (+++), en la mezcla de carbonatos. Ver figura en color en la web.

se observations point to the presence of traces of water bearing clay minerals such as montmorillonite and/or illite. Another alternative explanation for the strong band at 1900 nm is the presence of liquid water in microscopic fluid inclusions, which are very common in carbonates (Gaffey, 1984).

The main calcite feature has the maximum depth at 2335 nm (Hunt and Salisbury, 1971) (Fig. 4). This feature coincides in many of the pixels in the classified image, and it is depicted by yellow colour.

The position of the main dolomite feature at 2315 nm with a shoulder at 2275 nm is present in both the USGS spectral library and in sample spectra. It has been possible to distinguish minerals or mixtures with descending amounts of magnesium by seeing the change in position of the dolomite feature at 2315 nm to the main calcite feature at 2335 nm.

Conclusions

The spectral curves corresponding to different pixels of the studied rock sample show variations allowing to distinguish between calcite and dolomite, and variable proportions of calcite/dolomite mixture, which in the near future will be additionally validated through XRD and XRF diffraction analysis.

The fact that the base carbonate is calcite or dolomite does not present a major problem as long as the content of clays and other components as iron oxides do not exceed a certain amount, obscuring the carbonates absorption features.

Imaging spectroscopy proximal sensing procedures have a great potential for different geological applications helping to identify relevant minerals in different geological contexts as for instance, in the mining industry, in order to assess the quality of the product and evaluate deposit-specific geological materials before the extraction. The improvement of the Imaging Spectroscopy cutting-edge technology on the use hyperspectral proximal mapping algorithms and techniques to several geological applications

(drill-core analysis, vertical outcrops interpretation, etc.), in the context of natural resources optimizing and scientific knowledge improvement, represents a further challenge in this direction.

Contribution of the authors

I.R.: structure of the paper, methodology, figures, manuscript review, research/analysis. EGM: conceptualization, experimental design, structure of the paper, manuscript review, coordination, supervision. MFJ: structure of the paper, data acquisition, initial image treatment, manuscript review, coordination. WB: responsible of image acquisition, hardware and software configuration. JCM: rock sampling and geochemical analysis. AEG: rock sampling, methodology and field-work.

Acknowledgements

Research funded by Project HYPO-PROCKS (PDC2021-12352-100), MCIN/AEI/10.13039/501100011033 and the European Union "NextGeneration"/PTR, and project HYPERLANDFORM (PID2023-150229OB-100) by the Spanish Ministry of Science, Innovation and Universities-AEI.

The authors of this work acknowledge the effort and contribution of the manuscript reviewers.

References

- Alonso de Linaje, V. and Khan, D.S. (2017). *Sedimentary Geology* 353, 114-124. <https://doi.org/f99bqp>
- Baena, L., (1974). *Mapa Geológico de España 1:50000, Hoja Magna Jumilla* 869. Servicio Geológico y Minero de España.
- Bayly, J.G, Kartha, V.B. and Stevens W.H. (1963). *Infrared Physics* 3(4), 211-222. <https://doi.org/bnrc5p>
- Boesche, N.K., Rogass, C., Lubitz, C., Brell, M., Herrmann, S., Mielke, C., Tonn, S., Appelt, O., Altenberger, U. and Kaufmann, H. (2015). *Remote sensing* 7, 5160-5186. <https://doi.org/m8xz>
- Clark, R.N. (1999). *Manual of Remote Sensing, Volume 3, Remote Sensing for*

the Earth Sciences, John Wiley and Sons, New York, 3-58.

Gaffey, S.J. (1984). *Spectral reflectance of carbonate minerals and rocks in the visible and near-infrared (0.35-2.55 μm): Applications in carbonate petrology*. Ph.D. thesis, Honolulu, University of Hawaii, 236 p.

Goetz, A.F.H., Vane, G, Solomon, J. and Rock, B.N. (1985). *Science* 228, 1147-1153.

Hunt, G.R. (1977). *Geophysics* 42, 501-513. <https://doi.org/dbz3zs>

Hunt, G.R. and Salisbury, J.W. (1970). *Modern Geology* 1, 283-300.

Hunt, G.R. and Salisbury, J.W. (1971). *Modern Geology* 2, 23-30.

Jerez, L., García-Monzón, G., and Jerez, F. (1974). *Mapa Geológico de España 1:50000, Hoja Magna Calasparra* 890. Servicio Geológico y Minero de España.

Kokaly, R.F., Clark, R.N., Swayze, G.A., Livo, K.E., Hoefen, T.M., Pearson, N.C., Wise, R.A., Benzal, W.M., Lowers, H.A., Driscoll, R.L. and Klein, A.J. (2017). *USGS Spectral Library Version 7: U.S. Geological Survey Data Series* 1035, 61 p. <https://doi.org/ghw2cg>

Krupnik, D. and Khan, S. (2019). *Earth-Science Reviews* 198, 102952. <https://doi.org/gnkmj>

Kruse, F.A., Lefkoff, A.B., Boardman, J.B., Heidebrecht, K.B., Shapiro, A.T., Barloon, P.J. and Goetz, A.F.H. (1993). *Remote Sensing of Environment* 44, 145-163. <https://doi.org/csm2xm>

Murphy, R., Schneider, S. and Monteiro, S.T. (2014). *Remote Sensing* 6(9), 9104-9129. <https://doi.org/gcfkz8>

Riaza, A., García-Meléndez, E. and Mueller, A. (2011). *International Journal of Remote Sensing* 32(1), 185-208. <https://doi.org/cn9sd7>

Van Der Meer, F. (1995). *Remote Sensing Reviews* 13, 67-94. <https://doi.org/b4rq2h>

Zaini, N. (2018). *Infrared carbonate rock chemistry characterization*. Ph.D. thesis, Enschede, University of Twente, 129 p.

Zaini, N., van der Meer, F., and van der Werff, H. (2014). *Remote Sensing* 6(5), 4149-4172. <https://doi.org/gcfkxg>